Case Number: AA-1
Date: 31 January 2022

Patient History

Sawyer, an 8-year old male neutered Weimaraner, presented to the hospital with a history of right foreleg (RF) lameness over several months and a noticeable swelling on the posterior aspect of the leg just proximal to the carpus. The lameness occurred acutely while running off leash. The referring veterinarian prescribed a course of grapiprant[a] 60 mg once daily. No improvement in lameness was seen with medication, although rest did appear to improve the clinical lameness. The owner noticed periods of lameness off and on after that, usually related to exercise and play with other dogs. The dog was currently walking 2 to 3 km per day and using stairs, although slowly when lame. Radiographs performed by the referring veterinarian were normal other than demonstrating swelling in the tendons proximal to the accessory carpal bone. No previous traumatic episodes of lameness had occurred to the owner's knowledge other than developing hypertrophic osteodystrophy as a puppy for which he was prescribed prednisone.

On examination, Sawyer weighed 31.3kg and had a body condition score of 5/9. Vital signs were all normal. A mild RF lameness was noted in the clinic but was weight bearing well on the leg at stance.

Palpation of the myofascia revealed no generalized sarcopenia, and the cervical, thoracic and lumbar spine was comfortable and with normal mobility. No orthopedic abnormalities were noted in either hind leg or the left front leg. Lack of myofascial pain in the musculature of these limbs suggested chronic weight shifting from normal was not likely a concern.

Sawyer's RF leg revealed a slight drop in the carpus. The distal phalanges had slightly reduced tone to resist extension but had normal tone in the proximal phalanges, and none showed abnormal extension. Palpation of digits, metacarpals, and carpus was considered normal, with no increase in joint effusion, and no instability. The accessory carpal bone palpated in its normal position and was firmly attached. Proximal to the accessory carpal bone, the tendon of the flexor carpi ulnaris was firmly thickened but not painful to palpation. The swelling extended proximally 4 cm but palpation of the carpal and digital flexor muscle bellies was considered normal. Elbow and shoulder palpation revealed normal range of motion, and no myofascial atrophy, pain or swelling other than trigger points in the long head of the triceps muscle.

A tentative diagnosis of a strain to the flexor carpi ulnaris (FCU) tendon was offered pending further imaging.

---

[a] Galliprant, Elanco

Therapy included applying a medium carpal wrap[b], and twice weekly laser and therapeutic ultrasound treatments. Laser was applied with 6W for a total of 720 J[c]. Therapeutic ultrasound[d] was applied at 100%, 3MHz, 0.5 W/cm2 for 8 minutes. The owner was advised to continue with walks of the same length but avoid off-leash running and play.

On the fourth visit, the owner noted that Sawyer appeared to be benefitting from the treatments with the tendon appearing smaller and more subtle. Blood was taken for a complete blood cell count (CBC)[e] and chemistry panel[f] in advance of PRP therapy.

Three weeks after his initial assessment, Sawyer was admitted for diagnostic ultrasound of both forelegs and PRP therapy at the site of injury. He was administered 0.2 mg/kg butorphanol tartrate[g] and 0.05 mg/kg dexmedetomidine hydrochloride[h] intravenously. 50 mls of whole blood was collected from the jugular vein into a syringe containing 10 mls of ACD-A anticoagulant and prepared by a double centrifuge technique to provide 4 mls of platelet-rich plasma (PRP)[i].

Ultrasound was performed with a broad-spectrum linear matrix array ML6 – 15 probe[j] at 15 MHz. Following the ultrasound examination, 2 mls of prepared PRP was injected via a 22G, 3 cm long needle into the damaged region of the flexor carpi ulnaris tendon proximal to the accessory carpal bone on the RF leg.

The owner was instructed to maintain a carpal wrap for an additional 8 weeks on both forelegs during which and additional 6 therapeutic laser and ultrasound treatments were administered twice weekly. The owner was instructed to continue with walks but avoid off-leash activity.

A recheck was performed at 3 weeks post-PRP treatment. The owner had not noted any further episodes of lameness. The firm swelling was still evident in the flexor carpi ulnaris tendon; however, the carpus was now straighter with less carpal extension with weight bearing. Flexor tone had returned fully to all distal phalanges with Sawyer assuming a normal posture.

Two months after this last visit, Sawyer presented for lameness to the left foreleg (LF) of ten days duration. Sawyer has been kept on leash for walks and there had been no injury, slip or fall to account for the lameness. The owner had also continued to provide carpal support using carpal wraps on both forelegs. Upon examination, firm swelling and mild redness proximal to the accessory carpal bone was noted in the region of the FCU of the LF leg. The accessory

---

[b] Orthopets, Colorado
[c] K-laser, Eltech K-laser srl
[d] Intelect Transport Ultrasound, Chattanooga
[e] Pro-Cyte One Hematology Analyzer, Idexx Inc.
[f] Catalyst One Chemistry Analyzer, Idexx Inc.
[g] Torbugesic, Zoetis
[h] Dexdomitor 0.5mg/ml, Zoetis
[i] CRT PurePRPII, Companion Animal Health
[j] GE logic 10

carpal bone palpated as normal, digital flexor and extensor tone was normal as was position of the digits in standing. Carpal range of motion was normal, no instability or swelling was found, and no pain was observed on palpation. Sawyer was admitted for ultrasound of the injured region in the LF leg.

Laboratory Results

TEST	RESULT	UNITS	NORMAL RANGE	
			Low	High
RBC	7.43	x10^12/L	5.65	8.87
HCT	50.8	%	37.3	61.7
HGB	17.6	g/dL	13.1	20.5
MCV	68.4	fL	61.6	73.5
MCH	23.7	pg	21.2	25.9
MCHC	34.6	g/dL	32	37.9
RDW	18.4	%	13.6	21.7
%RETIC	1.5	%		
RETIC	**113.7**	**K/µL**	**10**	**110**
RETIC-HGB	26.2	pg	22.3	29.6
WBC	8.41	x10^9/L	5.05	16.76
NEU	5.59	x10^9/L	2.95	11.64
LYM	2.02	x10^9/L	1.05	5.1
MONO	0.44	x10^9/L	0.16	1.12
EOS	0.33	x10^9/L	0.06	1.23
BASO	0.03	x10^9/L	0	0.1
PLT	289	K/µL	148	484
MPV	11.5	fL	8.7	13.2

Table 1: Complete blood cell count

TEST	RESULT	UNITS	NORMAL RANGE	
			Low	High
GLU	6.17	mmol/L	3.89	7.95
CREA	90	µmol/L	44	159
UREA	3.3	mmol/L	2.5	9.6
BUN/CREA	9			
PHOS	**0.74**	**mmol/L**	**0.81**	**2.2**
CA	2.64	mmol/L	1.98	3
TP	69	g/L	52	82
ALB	35	g/L	22	39
GLOB	34	g/L	25	45
ALB/GLOB	1			
ALT	69	U/L	10	125
ALKP	**565**	**U/L**	**23**	**212**
GGT	5	U/L	0	11
TBIL	8	µmol/L	0	15
CHOL	7.11	mmol/L	2.84	8.26
AMYL	662	U/L	500	1500
LIPA	1519	U/L	200	1800
Na	152	mmol/L	144	160
K	4.5	mmol/L	3.5	5.8
Na/K	34			
Cl	116	mmol/L	109	122
Osm Calc	302	mmol/kg		

Table 2: Serum chemistry panel

Sonographic Images

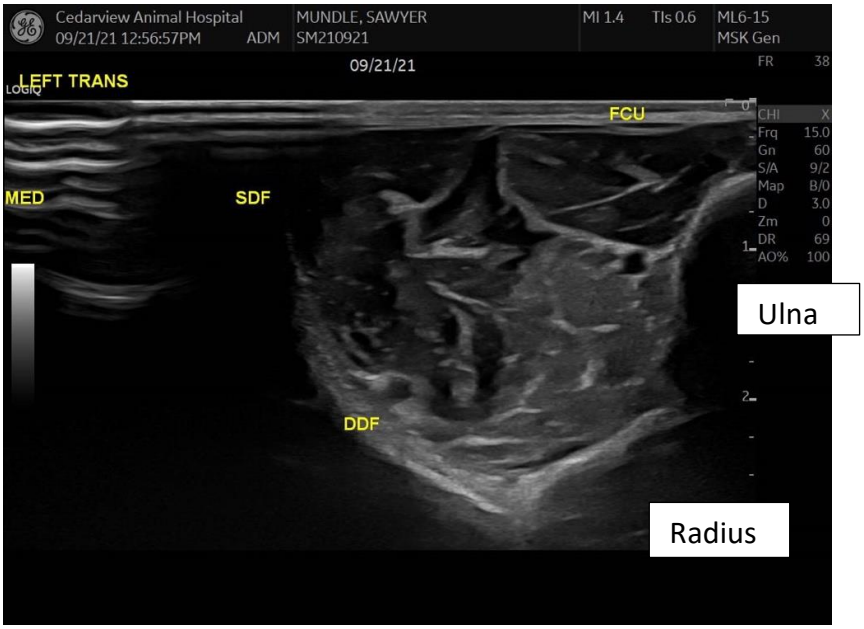

Image 1: Transverse image of the posterior aspect of the left (unaffected) antebrachium at time of initial examination. The image is taken from the posterior aspect of the leg (top of screen) and directed to the anterior aspect of the leg. The left side of the image points to the dog's medial aspect. The deep digital flexor (DDF) comprises the largest muscle belly at this site and sits deep to the medial superficial digital flexor (SDF) and the lateral flexor carpi ulnaris (FCU).

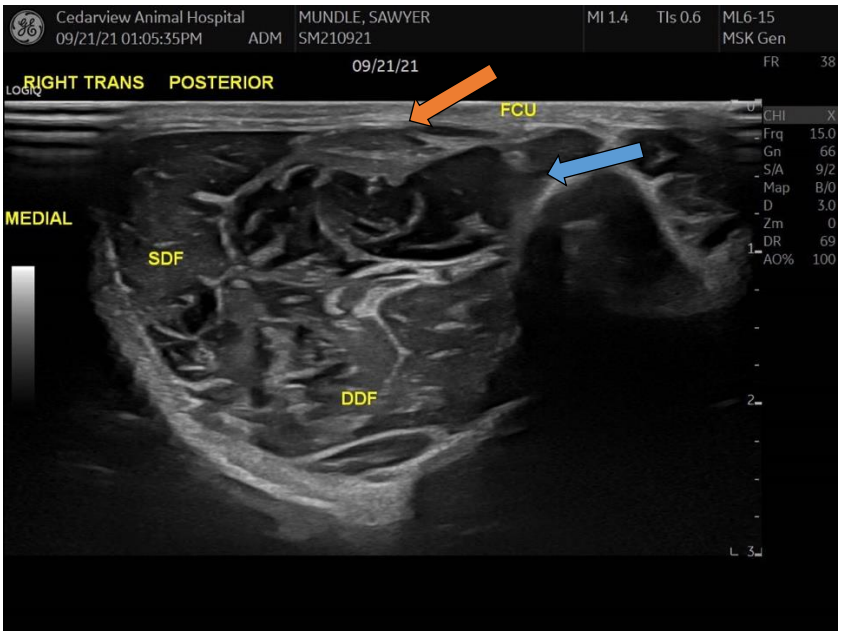

Image 2: The right (affected) foreleg seen in transverse at the same level and view as image 1. In a transverse view, the edges of the ulna and radius are seen as hyperechoic reflective solid lines with distal acoustic shadowing where sound beam incidence is perpendicular to the bone surface. Muscle is characterized as a mixture of low to medium echogenic tissue interspersed by hyperechoic curves and speckles of perimysial connective tissue within muscle bellies and between muscles[1].

The flexor carpi ulnaris muscle is composed of two heads, the ulnar and humeral, both inserting on the accessory carpal bone distally. The ulna head's muscle belly is shorter than the humeral head belly which continues distally. At this level, the orange arrow represents the tendon of the ulna head while the blue arrow shows the muscle of the humeral head.

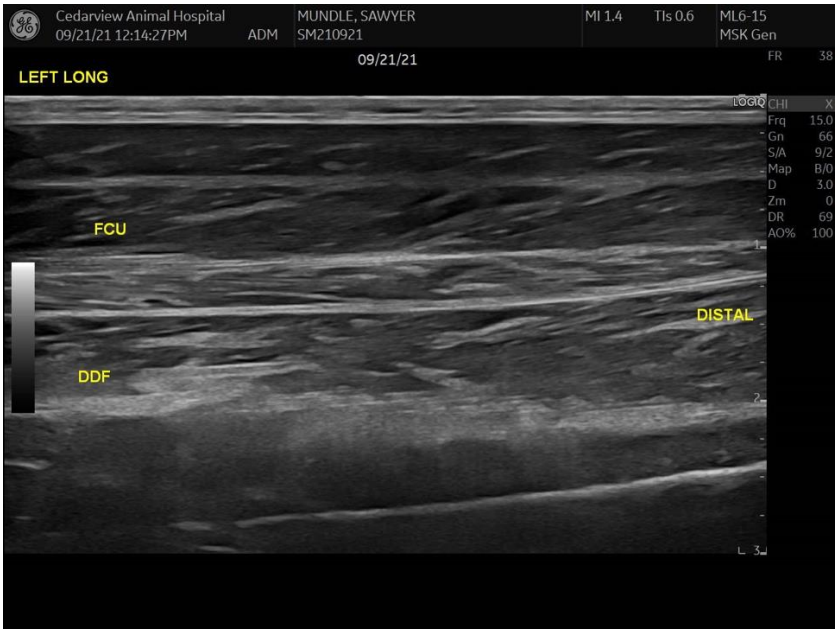

Image 3: Long axis view of the posterior (near field) aspect of the left antebrachium. From deep to superficial, the bright hyperechoic solid line represents the radius, over which the deep digital flexor lays. The next moderately hyperechoic line represents the junction between the flexor carpi ulnaris muscle overlying the DDF muscle. In the long axis view, the muscle appears hypoechoic with linear striations.

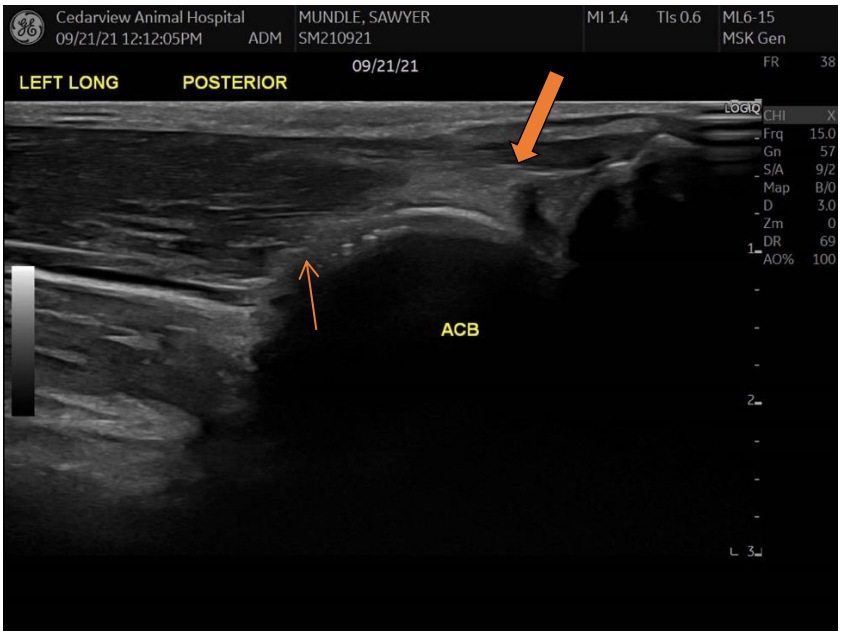

Image 4: Long axis view of the posterior aspect of the distal **left** antebrachium. The superficial FCU is noted to attach onto the accessory carpal bone (ACB). At this level, the FCU is a combination of the ulnar and humeral heads coming together in a tendinous unit. Normally, the tendon should show linear moderately echoic striations ending at a clean bony interface. The striated echoarchitecture is interrupted focally just proximal to the final accessory carpal bone (large arrow). The hypoechoic region just distal to the musculotendinous junction area indicated loss of normal tendon integrity. Very small hyperechoic foci are noted on the proximal edge of the ACB. At this level, the ulnar head tendon is deep to the larger humeral tendon and is seen here (smaller arrow)[2],[3].

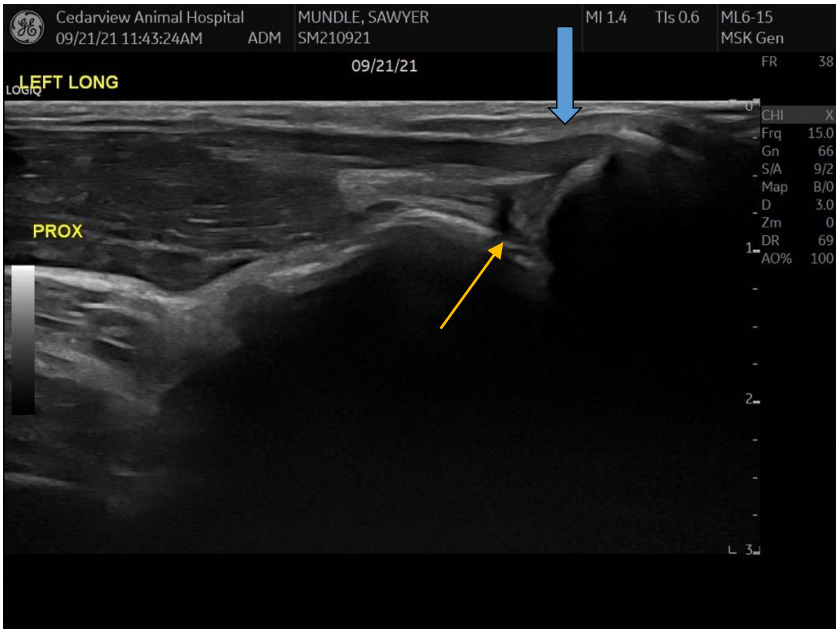

Image 5: Another long axis view of the distal FCU of the left foreleg. The blue arrow shows the attachment of the humeral head of the FCU. A hyperechoic region is seen within the distal radial head with focal loss of echoarchitecture and acute drop in echogenicity (yellow arrow).

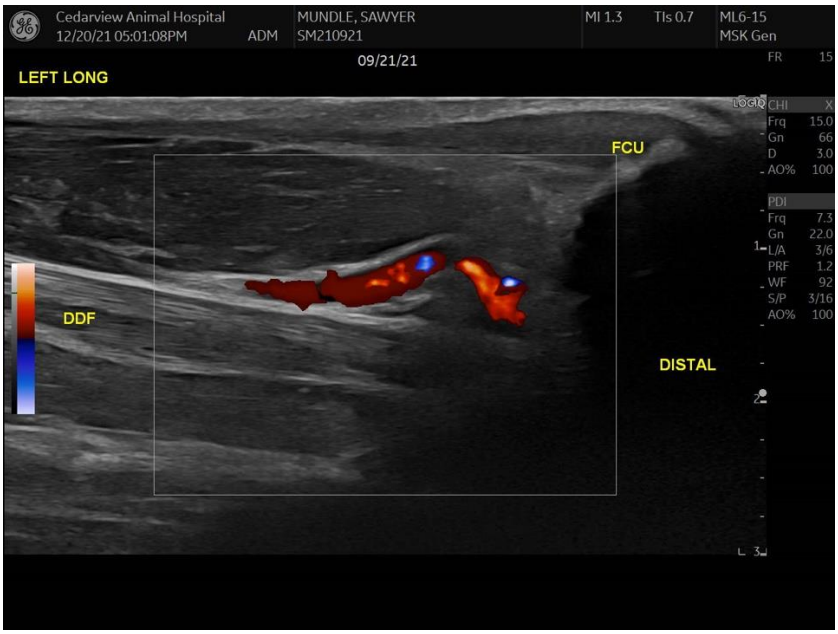

Image 6: In the mediopalmar view, colour flow doppler is applied to the region to highlight the blood vessels situated between the FCU and the deeper DDF tendons. These are the median and ulna arteries and assist in determining the anatomy of the tendon structures in this location.

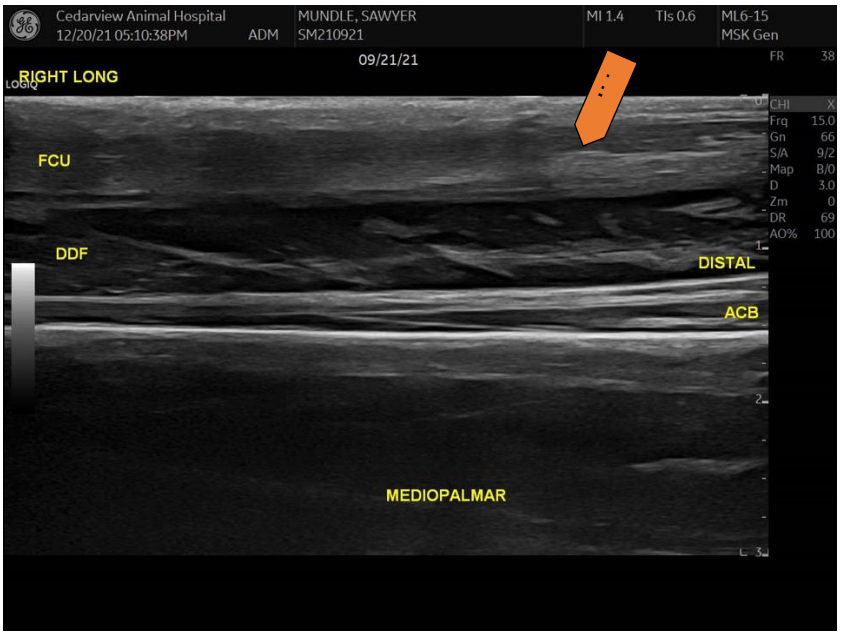

Image 7: A long axis medioposterior view of the right antebrachium just proximal to the ACB. The bright linear hyperechoic interface in the mid-field represents the bone surface of the ulna. The DDF muscle is superficial to this line is situated and then the FCU. There is loss of the hypoechoic muscle and echoic striations within the FCU (arrow).

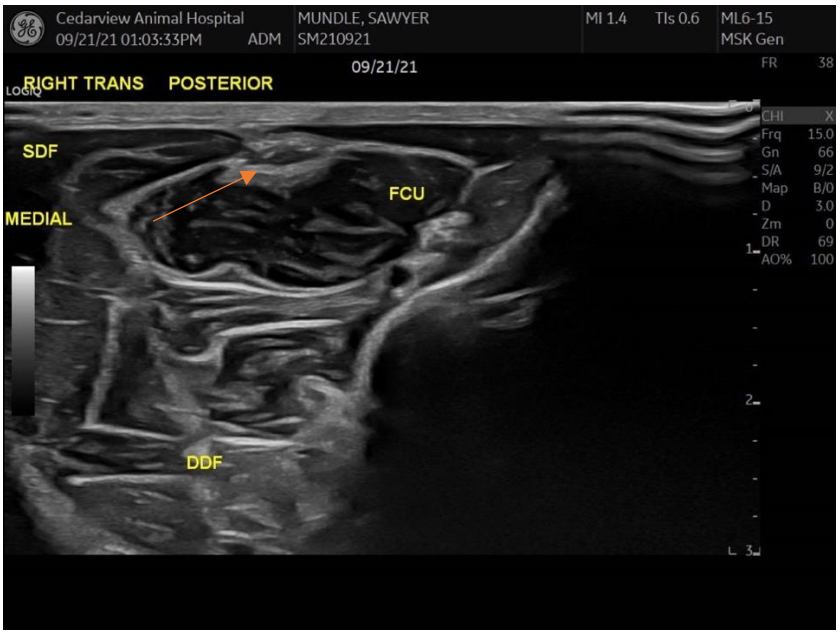

Image 8: Images 8 through 13 show transverse views of the palmar right antebrachium progressing from mid-radius/ulna distally. The ulnar head of the FCU (arrow) is superficial to the humeral head at this level but distally its tendon assumes a position deep to the humeral head tendon.

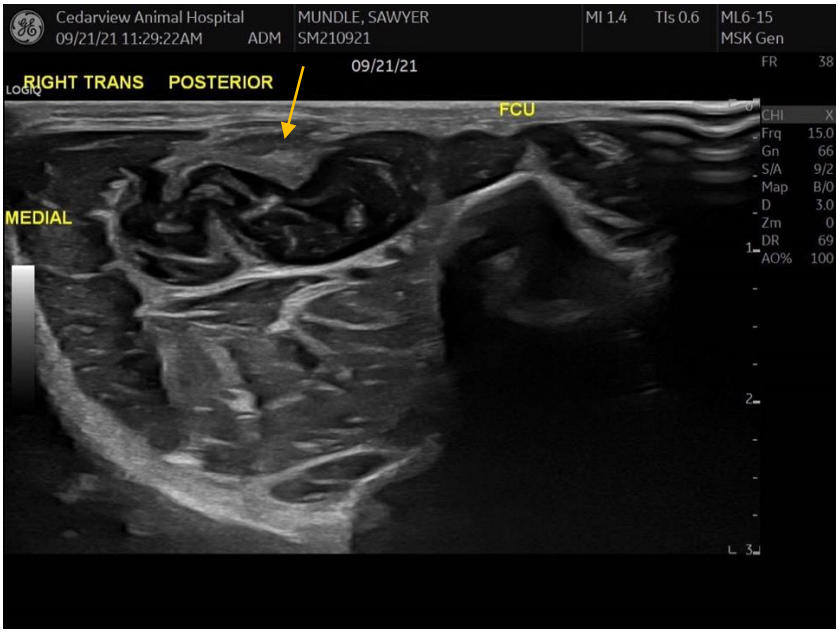

Image 9: Note an increase in more hyperechoic and homogenous tissue surrounding the ulnar tendon compared to the surrounding hypoechoic and normal humeral FCU muscle.

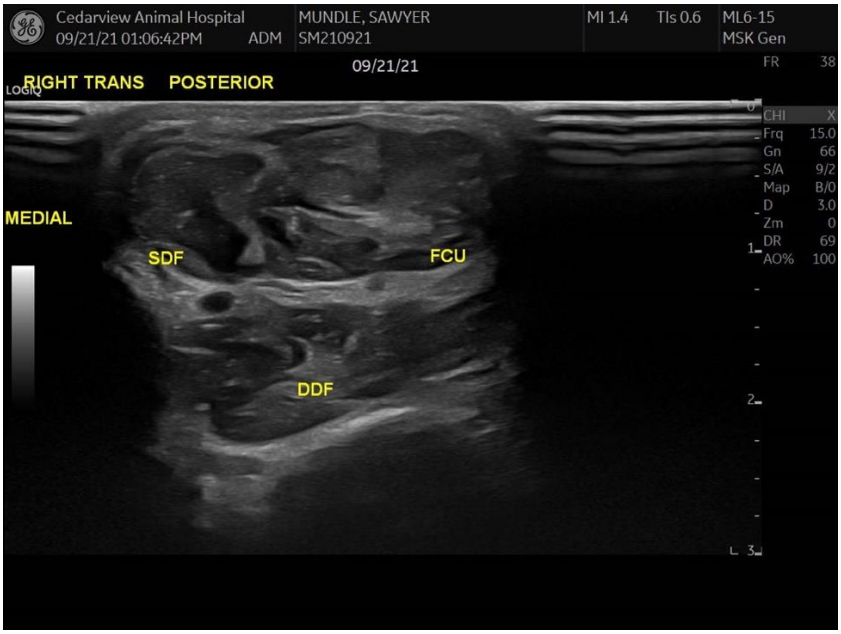

Image 10: A transverse view of the right posterior antebrachium. The vessels noted above can be seen as round hypoechoic structures within the fascia between the DDF and FCU. At this level, the FCU is losing its normal appearance and assuming a more dense and moderate echogenicity.

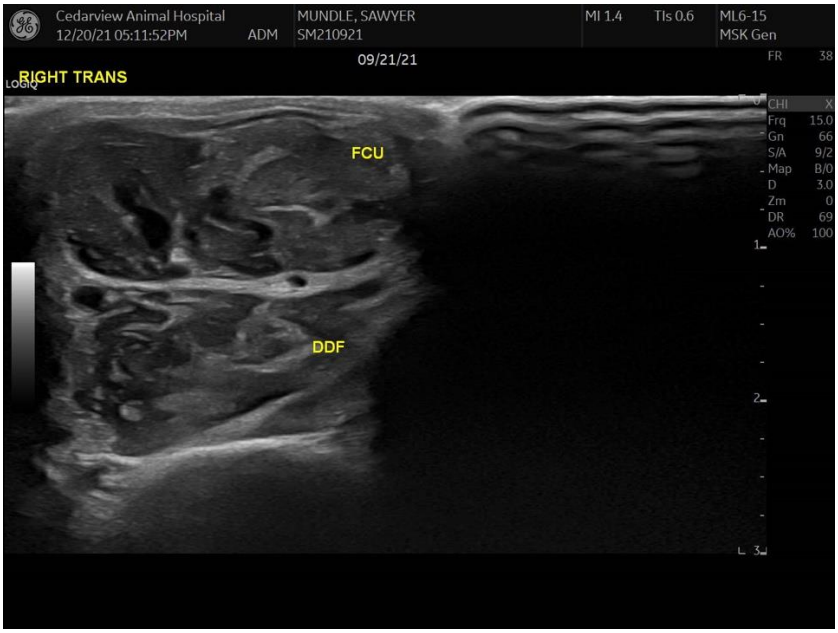

Image 11: Continuing distally on the right foreleg posterior transverse views, the FCU has become denser and more echogenic. An end-on vessel can be visualized in the brighter fascia between the FCU and deeper DDF.

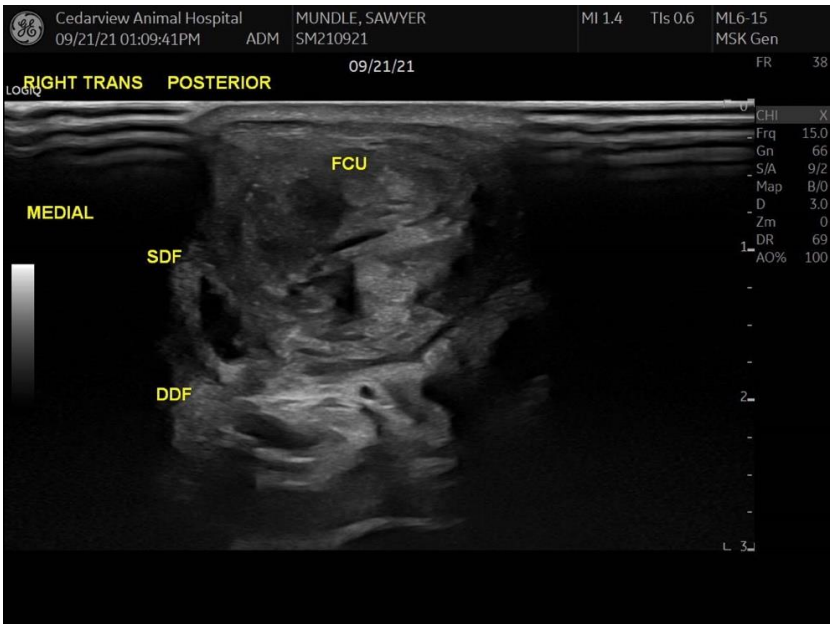

Image 12: Transverse view of the right posterior antebrachium just proximal to the accessory carpal bone. All posterior antebrachial muscles should be tendinous at this level, but it is difficult to distinguish the SDF and DDF tendons from the large mass that has developed at the tendinous part of the flexor carpi ulnaris. The anechoic end on vessel still permits orientation to the structure. The FCU tendons show as an enlarged mixed echogenic mass with anechoic regions interspersed between moderately and hyper-echoic tissue.

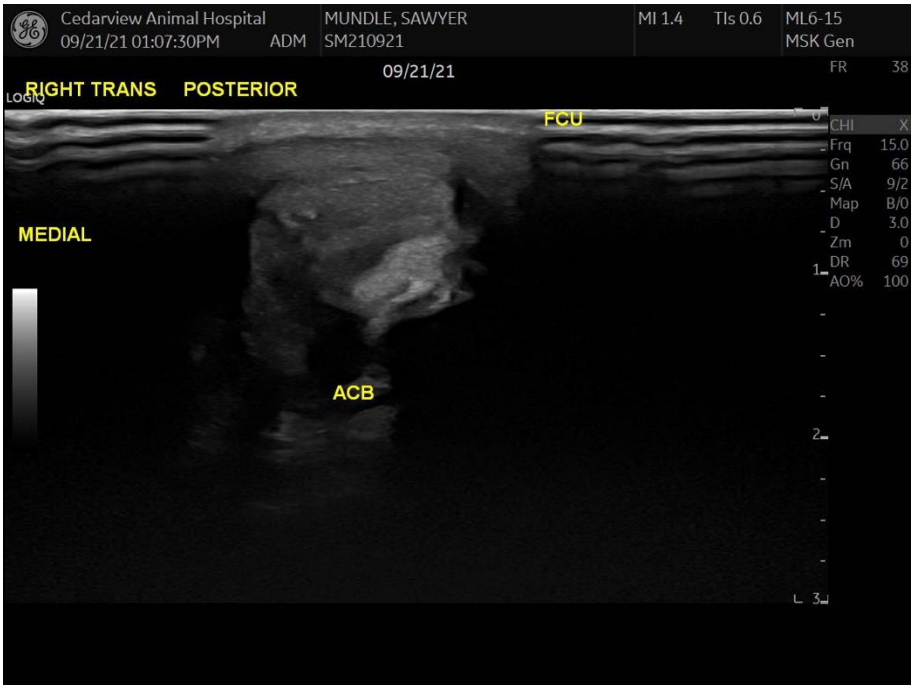

Image 13: Transverse posterior view of the right antebrachium at the level of the accessory carpal bone (ACB). The skin contact is narrowest at this point and shows a moderately homogenous and medium echogenic tissue between the echogenic interface of the bone and the skin.

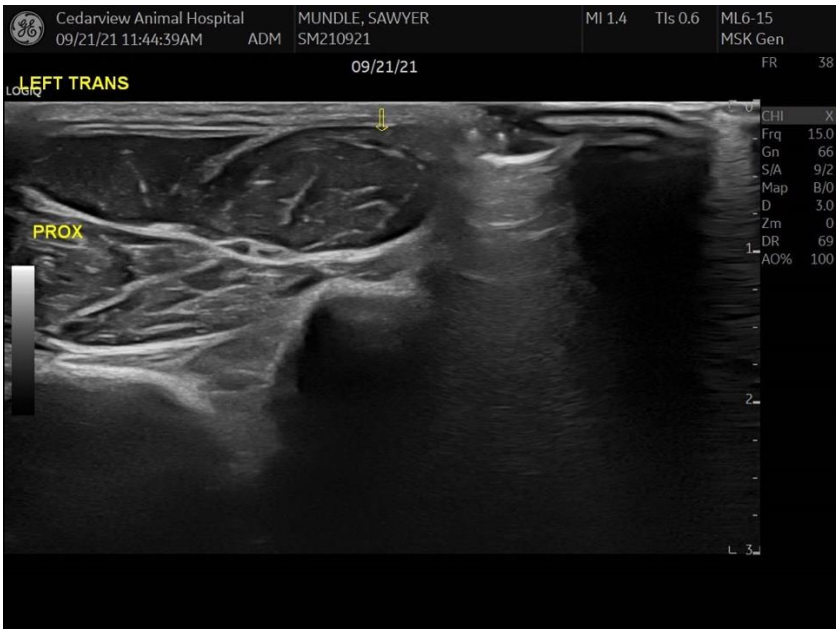

Image 14: A transverse view of the posterior aspect of the mid left antebrachium for comparison. The muscles hypoechoic to the surrounding fascia and contain brighter echoic striations from intramuscular connective tissue. The ulnar tendon is under the arrow.

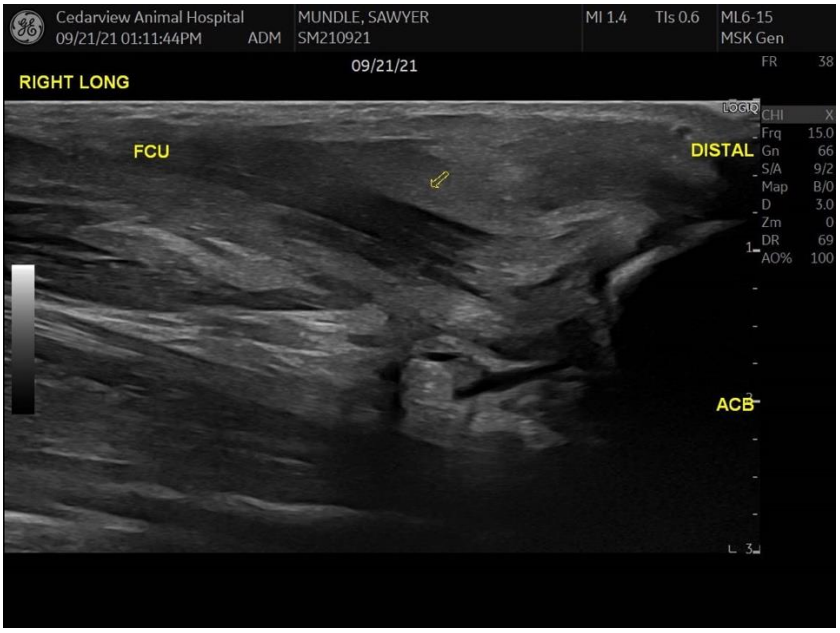

Image 15: Long axis view of the right posterior antebrachium. The left side of the image is directed proximally. A shadow cast by the ACB is seen on the right side of the image. Linear striations of FCU tendon can be seen extending from the left near field towards the ACB, but there is a loss of echogenicity at the level of the arrow. Closer to the transducer, the tissue is moderately echogenic and homogenous. Deeper to the tendon, the tissue appears disorganized and is more echogenic surrounding hypoechoic areas.

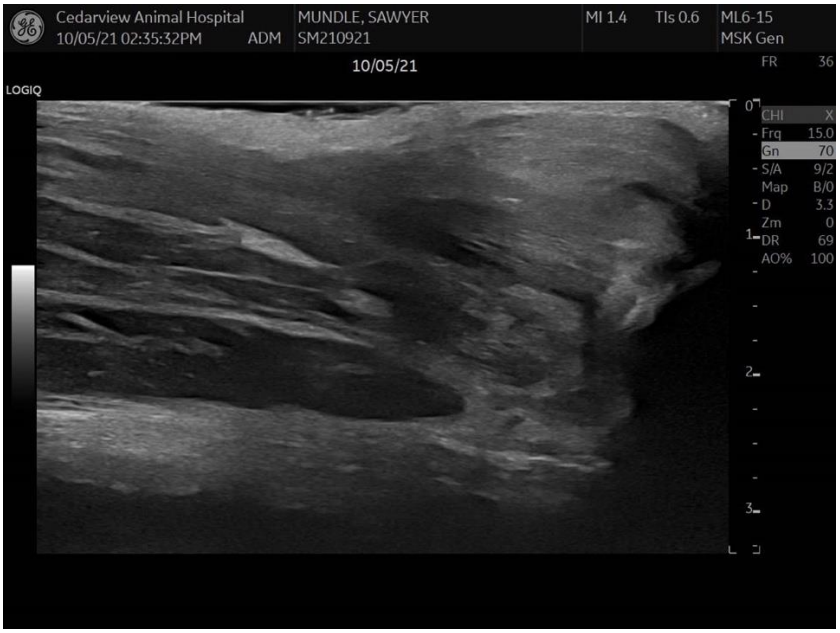

Image 16: Fanning the transducer medially and laterally over the swelling is performed to interrogate the lesion. In this view, the hypoechoic region in the FCU tendon is still visible surrounded by more echogenic and dense tissue, but the distal muscle belly of the DDF and SDF can be visualized on the left half of the image. Anistropy can cause decreased echogenicity in the tendon where the probe is not perpendicular to the structure, but adjacent areas of the tendon do not have this appearance despite a similar angle to the probe[4],[5]. There appears to be an area of acoustic enhancement on the right side of the image with slight edge shadowing and may be the result of altered skin contact along the image or improved ultrasound transmission over the swelling[4].

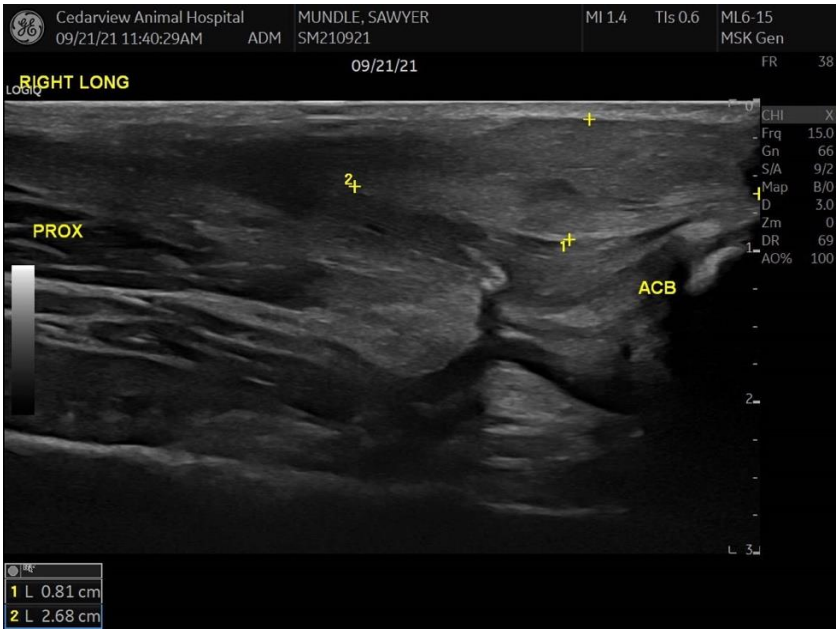

Image 17: Longitudinal view of the right distal FCU showing a region of almost homogenous moderate echogenicity measuring 2.7 cm in length and 0.8 cm in depth. The remnant ulnar FCU tendon appears to be displaced by this mass.

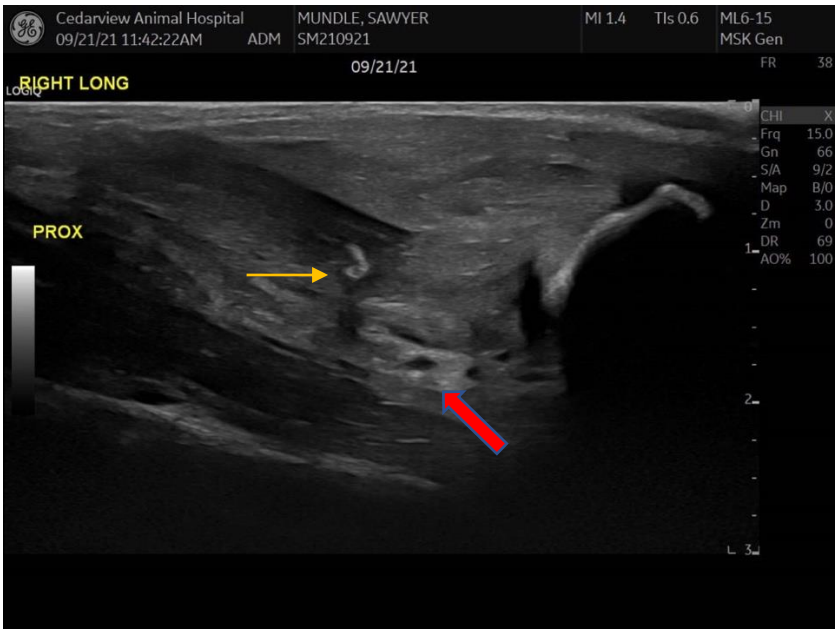

Image 18: Further long axis interrogation reveals as curled echogenic structure within the hypoechoic FCU region (yellow arrow). An acoustic shadow deep to the structure suggests that this is attenuating or reflecting the ultrasound waves and may represent calcification forming in the region of damage. A hypoechoic structure surrounded by hyperechoic tissue likely represent a blood vessel in the fascia between the FCU and DDF.

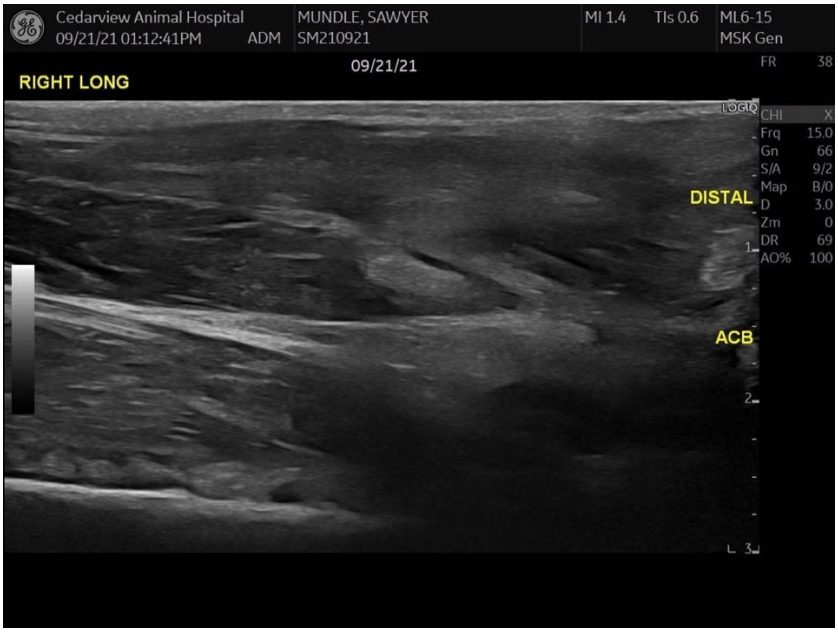

Image 19: Long axis view right posterior antebrachium. The transducer is moved slightly proximally on the leg to visualize the extent of diffuse echogenic changes associated with the FCU.

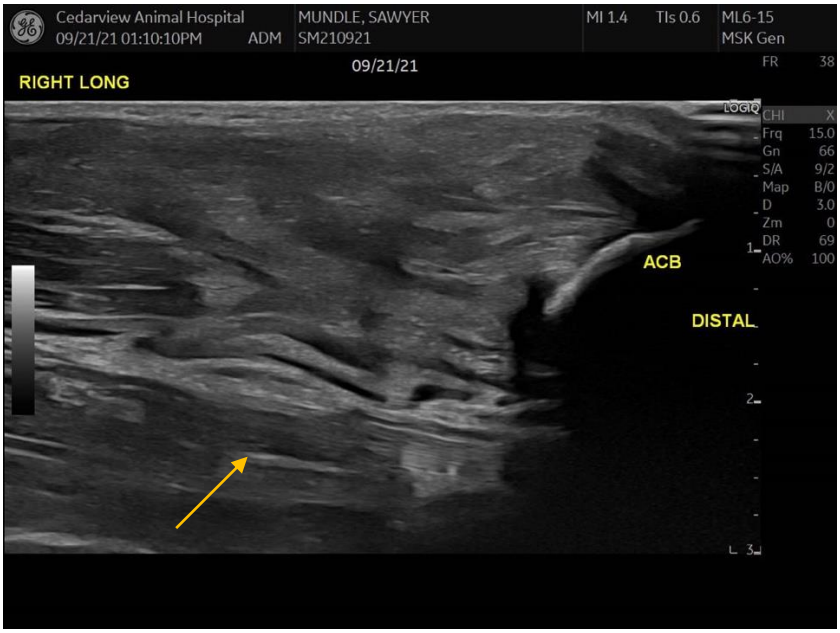

Image 20: Following the digital flexor muscles medially in this long axis view demonstrates normal linear intact tendons associated with the muscles deep to the intermuscular fascia (arrow).

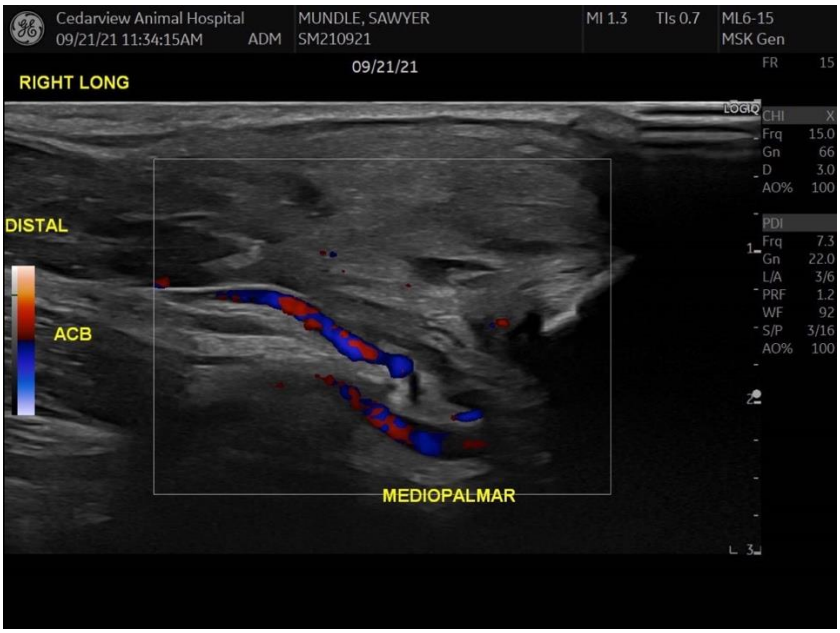

Image 21: Colour flow Doppler applied to the right leg confirms the separation of deep and superficial digital flexor tendons from the injured mass and also a lack of blood flow into the mass.

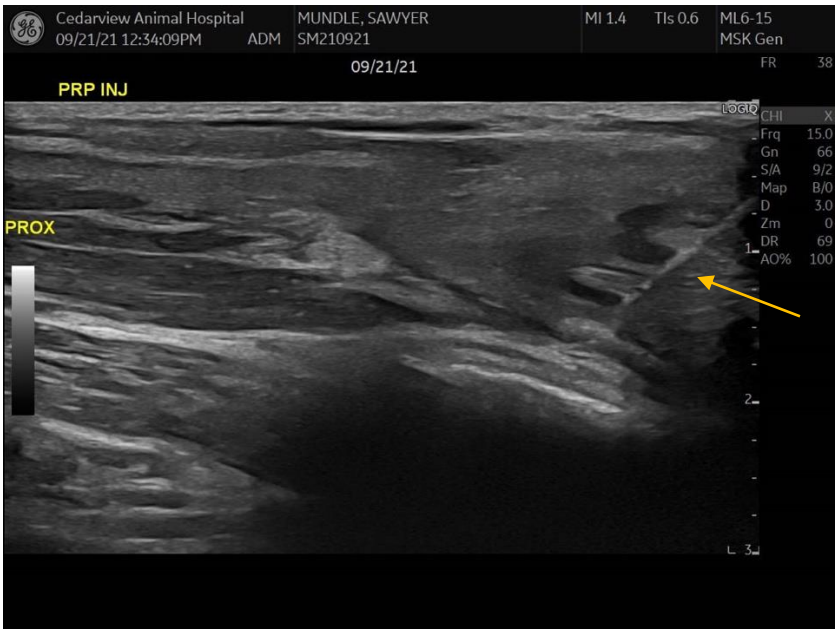

Image 23: A longitudinal view of the right posterior distal antebrachium during platelet-rich plasma injection (arrow). 2 mls of PRP was injected starting at a level just deep to the ulnar tendon and continued into the lesion as the needle was slowly retracted.

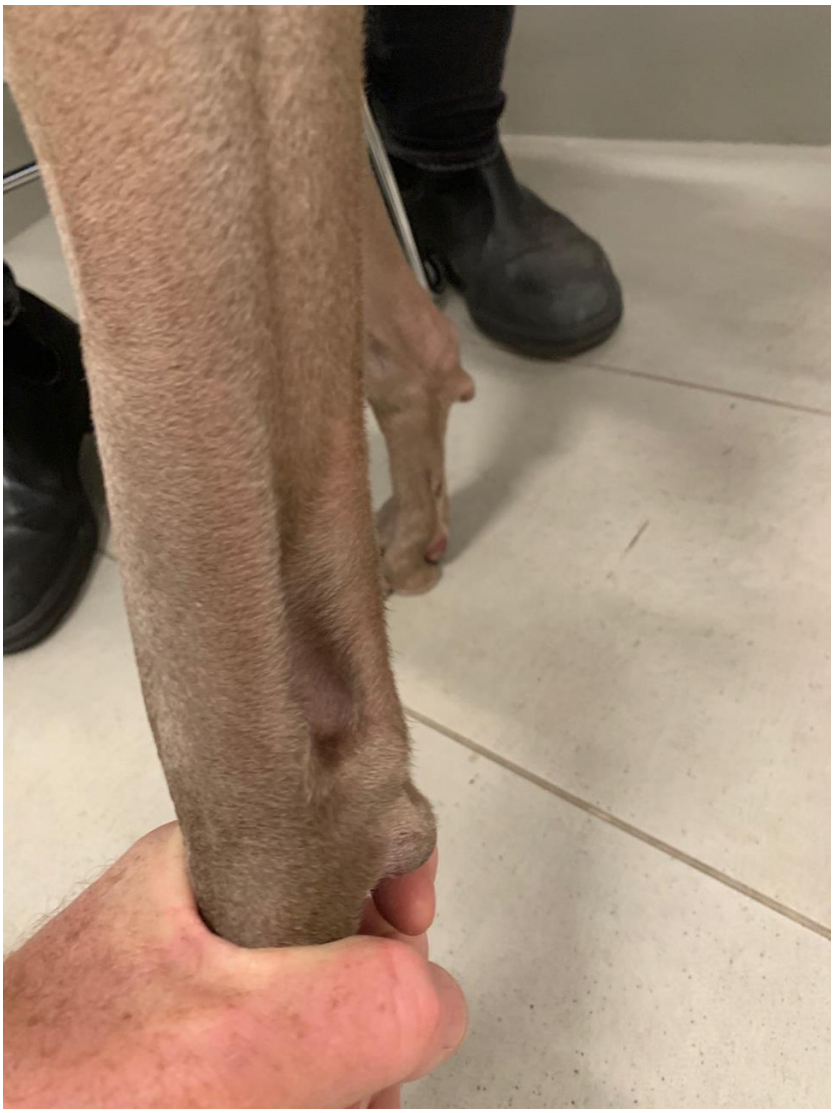

Image 24: Three weeks after the PRP injection, the dog presented with acute lameness to the left foreleg. Firm, non-painful swelling is evident in the distal flexor carpi ulnaris tendon. Note the right foreleg in the background showing an extended carpal position under load bearing. Residual swelling is still evident in the right flexor tendon.

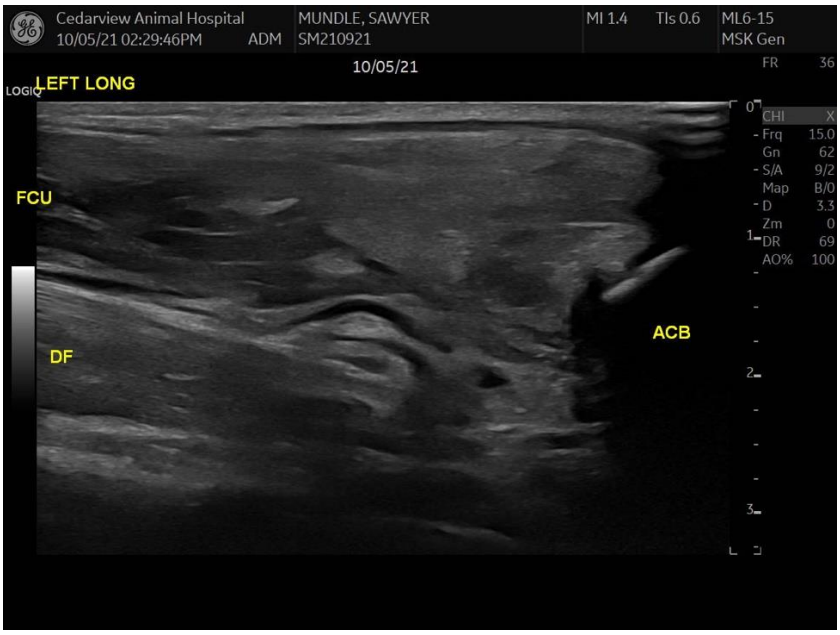

Image 25: Left foreleg long axis view of the palmar surface, distal antebrachium, three weeks after PRP treatment in the right foreleg. Compare to images 4 to 6 demonstrating the ultrasonographic changes because of injury. Digital flexor tendons are seen in the far field and are unaffected by trauma. The normal striated humeral head tendon has been replaced by a large moderately variable echoic mass. At the accessory carpal bone (ACB), the tissue has increased echogenicity with echogenic speckling. Deep to this attachment, an anechoic area can be seen, but it is not clear how much of this is affected by distal acoustic shadowing from the bone. In the proximal area of the image, striated ulnar head of the FCU can be visualized deep to a hypoechoic region.

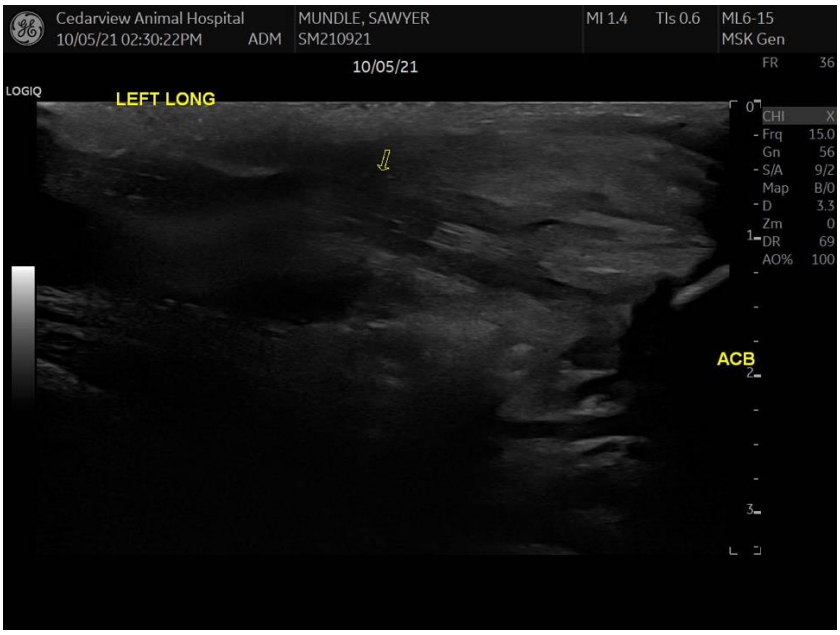

Image 26: Left foreleg long axis palmar view with the ulnar head tendon fibers visible in the deeper aspect of the tendon but with an area of hypoechogenicity (arrow), and anechoic area surround the tendon. Deep to the tendon, there is also a disorganized moderately variable echoic tissue.

Sonographic interpretation and differentials

- Chronic FCU musculotendinopathy in the right foreleg, and acute on chronic partial rupture in the left foreleg
    - Chronic moderate partial rupture of the right flexor carpi ulnaris tendon just proximal to the accessory carpal bone in exam 1. The alterations in tissue structure seen ultrasonographically likely represent fibrinous deposition and replacement within and surrounding the tendon injuries.
    - Chronic mild rupture noted in the left FCU initially with distal tendinous hyperechoic speckling, possibly indicating early mineralization in the tendinous attachments.
    - Acute partial rupture of the left flexor carpi ulnaris tendon just proximal to the accessory carpal bone in exam 2, three weeks after initial presentation. Anechoic areas likely represent edema or hemorrhagic fluid at the site of injury.
    - Intact deep and superficial digital flexor tendons in both forelegs. Both tendons in the right foreleg demonstrate some loss of normal hypoechoic appearance, presumably because of partial loss of function from the lameness.
    - No evidence for fracture or luxation of the accessory carpal bone.
    - Primary differential is a neoplasm of the peritendinous tissues (ie sarcoma). However, lack of blood flow into the mass suggests that this is not a neoplastic process.

Discussion

This paper demonstrates sonographic images of a chronic tendinopathy to the right flexor carpi ulnaris muscle and tendon in a Weimaraner and demonstrates the injection of PRP at the site of injury. In addition, it provides sonographic evidence for pre-symptomatic tendinopathy in the left FCU and then, three weeks later, images of an acute presentation of injury, providing ultrasound findings for three different clinical stages of tendinopathy.

Flexor muscles of the carpus and digits comprise the caudal antebrachial muscles of the dog: the flexor carpi radialis, flexor carpi ulnaris (FCU), superficial digital flexor (SDF) and the deep digital flexor (DDF). The flexor carpi ulnaris is composed of two heads, a smaller, flat ulnar head arising from the proximal ulna and a larger humeral head arising from the humeral medial condyle. The ulnar head is tendinous in the distal antebrachium, while the humeral head has a short tendinous insertion. Both heads insert on the accessory carpal bone, with the ulna tendon attaching independently and deep to the humeral head[2,6]. Both muscles are innervated by the ulna nerve and function to flex and abduct the paw.

Adjacent to this muscle are the SDF and the DDF, both of which function to flex the digits and the forepaw. The DDF lies deep to the FCU while the SDF is medial and superficial proximally. The tendons of the SDF and DDF muscles pass medially to the accessory carpal bone to insert on the palmar aspect of the second and third phalanges respectfully.

In the cat, and presumably the dog, the FCU muscle has been found to contain a high percentage of slow oxidative muscle fibers compared with other muscles of the foreleg, suggesting a dominant role in resisting gravity and aiding in stance[6].

Injuries to the flexor carpi ulnaris have been reported in athletic dogs, particularly racing Greyhounds[2,7]. There are no reports of prevalence of this injury in dogs in general, but there is one report of flexor carpi ulnaris sprain in a Weimaraner[2]. In that report, ultrasound findings revealed swelling around the tendon at the attachment to the accessory carpal bone presumed to be from inflammation, but with no involvement of the digital flexor tendons. Treatment involved splinting and a topical application of flumethazone and dimethyl suloxide, with complete resolution of the swelling and lameness 4 weeks after presentation.

Tendons contain Type 1 collagen within an extracellular matrix (ECM) arranged into parallel fibrils, fibers and fascicles along with small numbers of fibroblastic cells aligned in the same direction as the collagen fibrils. Water and non-collagenous proteins such as proteoglycans (PGs) between fibers and fascicles allow for sliding of fascicles over each other and tendon lengthening[8]. Along with Type 1 collagen, proteoglycans, and water, the ECM contains variable levels of elastin. The FCU is classified as an energy-storing tendon, aiding in weight-bearing and maintaining posture. For this purpose, these types of tendons contain higher concentrations of elastin compared to other tendon types (positional, wrap-around), which allows for elasticity and reversible deformation under load[3]. Under stress, provide durability and repeated cycles of elongation and recoil such as is needed in the FCU.

Normal tendon ultrasound reflects this fibrillar organization, seen as multiple tightly spaced parallel echogenic lines in the long axis[5]. In transverse, the ultrasound shows multiple echogenic dots. The tendon is uniform in texture and size.

Although often used interchangeably, tendinopathy refers to the clinical condition of tendon damage, while tendinosis reflects the histologic changes of degeneration. With tendinosis, normally flat tenocytes become activated and round, small PGs are replaced by large hydrophilic PGs which causes an increase in bound water and results in tendon thickening. Fibrillar disorganization ensues, causing a loss of parallel alignment and the area may develop neovascularization[8].

Healing of acutely damaged tendons progresses through several phases in a fairly predictable manner. Following acute injury there is an initial inflammatory phase from day 0 to approximately day 6 with hemorrhage, vasodilatory changes and increases in vascular permeability. White blood cells, platelets and cytokines are released into the inflammatory milieu causing clinical swelling and pain. This is followed by the reparative/proliferative phase in which a weak scaffold is developed of fibrin, fibroblasts are activated and angiogenesis in stimulated. The maturation or remodelling phase follows and may last weeks to months in which time the tendon regains strength and collagen fibrils realign with loading forces. Persistence of disorganized tissue or repeated episodes of damage and inflammation will prevent the tendon from regaining original strength and elasticity.

Ultrasound evaluation for damaged tendons is a diagnostic tool of choice for a number of reasons. The axial resolution for a 10 MHz probe is ~150 μm compared to MRI with an average slice thickness of 1 mm (high field MRI) and 3 mm slice thickness (low field MRI) [5]. Ultrasound is less expensive than MRI, can often be provided without anesthesia or sedation, and allows for dynamic visualization of the tendon under various loads and movement. In addition, it can be used for real-time guidance of injections into the tendon and Doppler evaluation can aid in assessment of vascularization. In humans, ultrasound has excellent accuracy (0.63 – 0.80) and sensitivity (0.68 – 0.87) compared to MRI in detecting clinical tendinopathy[8]. Despite that, it is still limited in its ability to differentiate partial tears from local degenerative changes. Furthermore, a tendon can appear normal sonographically but still have histologic changes. MRI can demonstrate edema and active perfusion and hence – despite some overlap between the modalities they contribute complementary information.

Ultrasound findings consistent with acute tendon damage include loss of the normal fibrillar pattern, hypoechogenicity, and tendon thickening[5]. In addition, peritendinitis may be revealed with thickening of the tendon sheath and fluid around the tendon[8]. Description of the ultrasound findings associated with the flexor carpi ulnaris tendon in dogs specifically is limited[2]. However, more information is reported for Achilles's tendon (AT) injuries and likely can be extrapolated to the FCU. For AT injuries, breed predispositions have been recorded with Dobermans, Border collies and Labrador retrievers[9]. Whether this predisposition occurs due to differences in tendon strength as a result of biochemical and mechanical properties, or from

structural susceptibility related to conformation is not apparent, but none of these breeds appear to be more susceptible to FCU damage. However, proposed general predisposing factors include obesity, diabetes, hyperadrenocorticism, corticosteroids and non-steroidal anti-inflammatory drugs[10]. Of interest is a reported predisposition in Doberman dogs to relative shortening of the flexor carpi ulnaris in skeletally immature puppies resulting in flexural deformity[11]. Additionally, fluoroquinolone use is associated with an increased risk of tendinopathy in people and rat models[12]. This dog had been diagnosed with hypertrophic osteodystrophy (HOD) as a puppy, for which it was treated with corticosteroids. Whether the HOD itself or subsequent treatment with corticosteroids predisposed Sawyer to subsequent FCU injury is unknown.

Descriptions of ultrasound findings for acute AT damage include the previously mentioned discontinuity of fibrillar patterns, with the ends of the tendons seen as hyperechoic and inhomogeneous. Between these ends, a heterogenous and irregular, hypoechoic to anechoic region exists representing a hematoma. With partial rupture, normal fibrillar patterns exist in non-injured tissue but areas of damage lose their normal echogenicity, become hypoechoic to anechoic and have heterogenous patterns[10].

In the first two weeks after damage, the hypoechoic hematoma becomes inhomogeneous, develops echogenic regions, and increases in thickness[13]. After eight weeks, as the healing progresses, the inhomogeneity decreases as does the tendon diameter. Fibrillar patterns begin to reappear to a maximum of twelve weeks after injury, however it can remain hyperechoic to the normal tendon for over a year.

Chronic, recurrent damage, conversely, can be seen as areas that become homogenous to highly non-homogenous and hypoechoic to hyperechoic to normal tendon, frustrating the ability to predict time from injury. Consider that these findings are supported by traditional 2-D imaging techniques, but with newer 2-D and 3-D imaging techniques, such as strain elastography and Doppler investigations, structural changes can be still seen at twenty four weeks post-injury and full restoration of tendon strength may take years[14].

Current research into tendinopathies in humans has resulted in the development of a continuum model of tendinopathy to explain the progression of tendon changes seen in damaged states, at a histological but also at an imaging and a clinical level[15]. The older view of a tendinopathy being seen as a progression from a trauma-induced inflammatory stage to a failed healing is now considered as a degenerative state with minimal clinical inflammation that fails under chronic stress or sudden loading.

The current model proposes that the early changes seen in tendon damage are non-inflammatory proliferative tissue reactions to overload or acute compression. Histologically, this is evidenced by an upregulation of proteoglycans and an increase in bound water, resulting in tissue thickening. Disrepair occurs matrix breakdown, collagen separation, growth of abnormal tenocytes and increases in tendon neovascularity[15]. While these stages are

reversible, continued collagen disruption, cell death (apoptosis), and ingrowth of vessels and nerves leads to irreversible changes and chronic clinical pain syndromes. Previous models did not adequately correlate the histological changes with that of clinical or imaging findings and this remains a challenge with describing sonographic images in the context of damage and prognosis.

Traditional 2-D imaging studies for tendon damage in humans provide conflicting results on the correlation of imaging changes and development of pain, for example. Furthermore, it is not possible to differentiate between asymptomatic versus symptomatic findings with imaging. While these limitations exist, it may be that many sonographic studies examine heterogenous populations with varying degrees of tendon degeneration, and more targeted approaches will benefit interpretation and therapy[15]. In this study, for example, the sonographic images suggested early asymptomatic degenerative changes in the left flexor carpi ulnaris tendon, which then became acutely damaged. Of interest would be whether treatment can be directed at this pre-symptomatic stage, either through rehabilitation therapies or regenerative medicine therapies (ie PRP) to prevent progression in damage.

The use of platelet-rich plasma for the treatment of tendinopathies follows a burgeoning understanding of the biochemical events involved in tendon damage and repair. Platelets are rich in over 300 described proteins stored in α-granules, dense granules and lysosomes, many of which have been elucidated as growth factors, including platelet-derived growth factor (PDGF), transforming growth factors (TGF), fibroblastic growth factor (FGF), endothelial growth factor (EGF), hepatocyte growth factor (HGF), and connective tissue growth factor (CTGF), among others. In addition to platelets and plasma signalling proteins, PRP also contains structural proteins such as fibrin and fibronectin that provides a scaffold for cellular adhesion and growth. Investigations into PR-therapies demonstrate modification of cell death, alterations in angiogenesis, and control of inflammation and pain through these biochemical influences[16].

In dogs, as with humans, evidence for or against benefits of PRP has been hampered by lack of standardization of different products and the quality of studies performed. However, there is compelling evidence being generated for the use of PRP as a therapy for tendon healing. For example, in a placebo-controlled experimental study in horses, surgical damage to the superficial flexor tendon was shown to have improved biochemical, biomechanical and histologic tissue properties 24 weeks after injury in tendons treated with a single injection of PRP compared to saline[17]. Additionally in animals, PRP has been shown to increase the myogenic precursor cell population necessary for myofiber formation.

The lameness that occurred in the right front leg had already progressed through the healing phases by the time the dog was presented, but persistence of lameness suggested that either the tendon was becoming further injured with activity despite attempts by the body to repair it, or that the injury itself was related to the development of a chronic pain state.

In this dog, the right foreleg FCU distal swelling measured at least 2.7 cm in length and 0.8 cm in thickness, and the normal striated tendinous structures had been replaced by moderately echogenic and homogenous tissue. The region had minimal anechoic areas that would be suggestive of edema or hemorrhage, expected with a more acute tendon injury. In addition, hyperechoic foci suggest mineralization within the damaged tendon.

The left foreleg initially presented with mild loss of normal tendon structure in the distal FCU and mild hyperechoic speckling at the attachment to the ACB, but three weeks later, the region was thicker and had areas of hypo and anechoic changes suggestive of fluid, with loss of tendon structure integrity.

Ultrasonographic images of the right foreleg, therefore, would likely represent a chronic state of injury. Interestingly, the left foreleg was imaged at the same time to provide a comparison to a "normal" tendon, and it revealed suspicious regions of echogenic variability suggestive of mild tendon abnormalities. The subsequent presentation of a left foreleg lameness revealing acute damage to the flexor carpi ulnaris provides an interesting sequence of sonographic images of tendon damage in various stages of damage and repair.

References

1. Themes UFO. Ultrasound of Muscle. Radiology Key. Published January 22, 2016. Accessed December 23, 2021. https://radiologykey.com/ultrasound-of-muscle/

2. Kuan S, Smith B, Fearnside S, Black A, Allan G. Flexor carpi ulnaris tendonopathy in a Weimaraner. *Aust Vet J*. 2007;85(10):401-404. doi:10.1111/j.1751-0813.2007.00187.x

3. Zink MC. *Canine Sports Medicine and Rehabilitation*. 2nd ed. Wiley-Blackwell; 2018.

4. Penninck D, d'Anjou MA. *Atlas of Small Animal Ultrasonography*. 2nd ed. John Wiley & Sons; 2015.

5. Lee KS. Musculoskeletal Sonography of the Tendon. *J Ultrasound Med*. 2012;31(12):1879-1884. doi:10.7863/jum.2012.31.12.1879

6. Evans, Howard E., de Lahunta, Alexander. *Miller's Anatomy of the Dog*. 4th ed. Elsevier, Saunders; 2013.

7. Duerr F, ed. *Canine Lameness*. Wiley-Blackwell; 2020.

8. Docking SI, Ooi CC, Connell D. Tendinopathy: Is Imaging Telling Us the Entire Story? *J Orthop Sports Phys Ther*. 2015;45(11):842-852. doi:10.2519/jospt.2015.5880

9. Corr SA, Draffan D, Kulendra E, Carmichael S, Brodbelt D. Retrospective study of Achilles mechanism disruption in 45 dogs. *Vet Rec*. 2010;167(11):407-411. doi:10.1136/vr.c4190

10. Abako J, Holak P, Głodek J, Zhalniarovich Y. Usefulness of Imaging Techniques in the Diagnosis of Selected Injuries and Lesions of the Canine Tarsus. A Review. *Animals*. 2021;11(6):1834. doi:10.3390/ani11061834

11. Whitelock R. Conditions of the carpus in the dog. *In Pract*. 2001;23(1):2-13. doi:10.1136/inpract.23.1.2

12. Melhus A. Fluoroquinolones and tendon disorders. *Expert Opin Drug Saf*. 2005;4(2):299-309. doi:10.1517/14740338.4.2.299

13. Kramer M, Gerwing M, Michele U, Schimke E, Kindler S. Ultrasonographic examination of injuries to the Achilles tendon in dogs and cats. *J Small Anim Pract*. 2001;42(11):531-535. doi:10.1111/j.1748-5827.2001.tb06022.x

14. Ryan M, Bisset L, Newsham-West R. Should We Care About Tendon Structure? The Disconnect Between Structure and Symptoms in Tendinopathy. *J Orthop Sports Phys Ther*. 2015;45(11):823-825. doi:10.2519/jospt.2015.0112

15. McCreesh K, Lewis J. Continuum model of tendon pathology - where are we now? *Int J Exp Pathol*. 2013;94(4):242-247. doi:10.1111/iep.12029

16. Andia I, Sanchez M, Maffulli N. Tendon healing and platelet-rich plasma therapies. *Expert Opin Biol Ther*. 2010;10(10):1415-1426. doi:10.1517/14712598.2010.514603

17. Bosch G, Moleman M, Barneveld A, van Weeren PR, van Schie HTM. The effect of platelet-rich plasma on the neovascularization of surgically created equine superficial digital flexor tendon lesions. *Scand J Med Sci Sports*. 2011;21(4):554-561. doi:10.1111/j.1600-0838.2009.01070.x